

## Recombination dynamics of exciton and exciton complexes in single quantum dots

This article has been downloaded from IOPscience. Please scroll down to see the full text article.

2010 J. Phys.: Conf. Ser. 210 012014

(<http://iopscience.iop.org/1742-6596/210/1/012014>)

[The Table of Contents](#) and [more related content](#) is available

Download details:

IP Address: 150.244.118.30

The article was downloaded on 26/03/2010 at 10:49

Please note that [terms and conditions apply](#).

# Recombination dynamics of exciton and exciton complexes in single quantum dots

M. D. Martín<sup>1</sup>, M. Martínez-Berlanga<sup>1</sup>, L. Viña<sup>1</sup>, B. Pietka<sup>2</sup>, and M. Potemski<sup>2</sup>

<sup>1</sup>SEMICUAM, Dept. Física de Materiales, Universidad Autónoma de Madrid, E-28049 Madrid, Spain

<sup>2</sup>Lab. National des Champs Magnetique Intenses (CNRS UPR3228), Université Joseph Fourier-Grenoble, F-38042 Grenoble-Cedex, France

e-mail: dolores.martin@uam.es

**Abstract.** We have studied the relaxation dynamics of excitons and exciton complexes in a single quantum dot using time-resolved photoluminescence. To avoid any interference of carrier diffusion and trapping we have excited the dot with energies below that of the wetting layer. The times extracted from a quantitative analysis are thus related only to the relaxation of carriers inside the dot. Since the dot is rather large it is possible to observe the recombination of carriers from different atomic shells. We observe a retardation of the carrier relaxation increasing excitation power due to the large number of charges filling the dot.

## 1. Introduction

Semiconductor quantum dots (QDs) offer the possibility to confine carriers in all three spatial directions, leading to fully discrete energy levels. They are one of the most suitable candidates to develop solid-state single-photon sources [1]. The study of carrier relaxation inside the QD is usually “contaminated” by carrier diffusion and/or trapping, since the excitation of the system is often made at wetting layer energies. Hence the long decay times (in the ns range) associated with QDs [2]. In the present work, we avoid the interference of relaxation and trapping by resonant excitation of the dot’s high energy shells.

## 2. Sample and experiment

The sample under study is a type II GaAs/AlAs double quantum well. The GaAs dots are formed by imperfections during the growth process (Ga segregation). The GaAs/AlAs structure is replaced by a GaAs/Al<sub>x</sub>Ga<sub>1-x</sub>As sequence ( $x < 0.33$ ). Due to the different sizes (tens of nanometers) and Al concentration, the dot emission energies spread over a broad energy range. The dot density is as low as  $10^6 \text{ cm}^{-2}$  and the very strong 3D confinement allows the observation of many multi-excitonic complexes.

The sample is kept at 10 K inside a cold finger cryostat and is optically excited with 2 ps-long pulses obtained from a Ti:Al<sub>2</sub>O<sub>3</sub> laser, tuned at 740 nm and spectrally filtered with an interference filter. The laser is focused to  $\sim 1 \mu\text{m}$  spot on the sample surface via a 50× microscope objective, mounted on 3 motorized translation stages, which is also used to collect the QD photoluminescence (PL). The PL is then filtered with an edge filter (cut at  $\lambda = 752 \text{ nm}$ ) placed in front of a spectrograph.

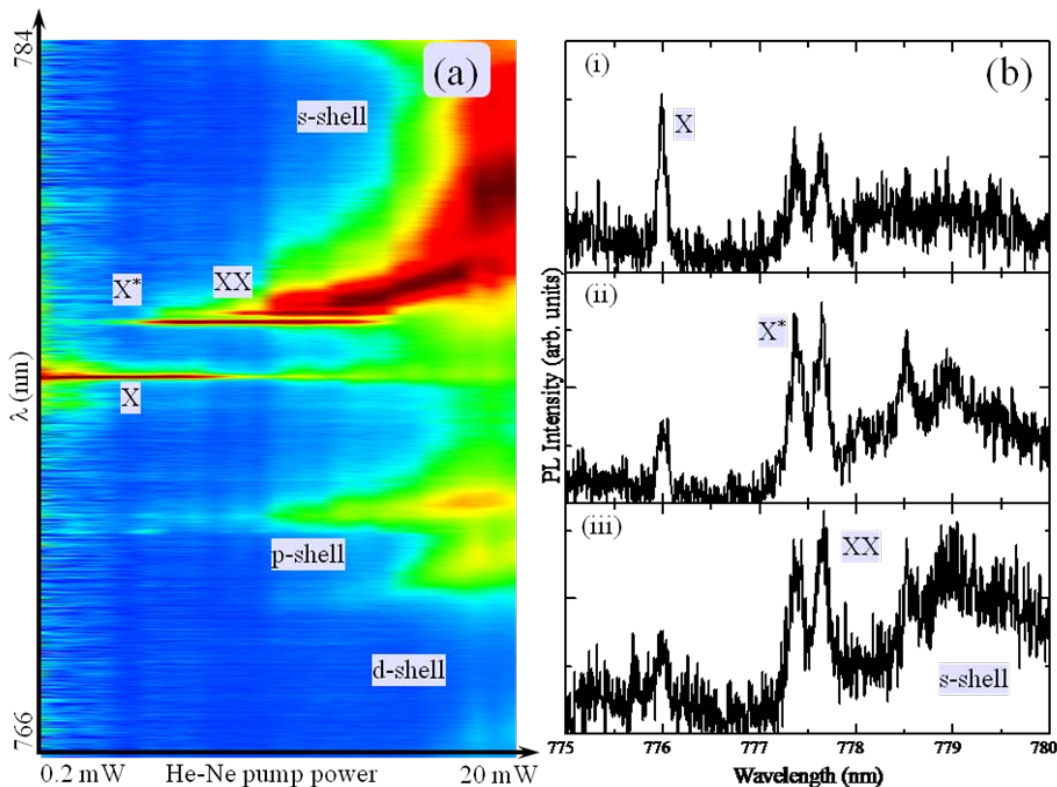


**Figure 1.-** (a) HeNe excited QD-PL as a function of pump power. The exciton (X), trion ( $X^*$ ), biexciton (XX), and the s, p and d-shells are clearly identified. (b) Time-integrated QD-PL obtained from streak camera images corresponding to (i) 32, (ii) 105 and (iii) 200  $\mu$ W Ti:Al<sub>2</sub>O<sub>3</sub> laser power.

The time-integrated PL is detected with a standard CCD and the time-resolved PL is detected with a streak camera (photon counting mode) with a time resolution of  $\sim 50$  ps.

Above a certain excitation power the position of the excitation spot over the QD drastically modifies the appearance of the PL spectra. This is due to the different carrier densities created inside the dot when the central part of the spot or the wings of its gaussian profile spatially overlap with the QD. In the first case it is the trion ( $X^*$ ) emission that dominates the PL, consistently with a higher excitation power (i.e. a large carrier density). In the later case it is the exciton (X) emission that displays the largest emission intensity since there are not enough extra charges to form the  $X^*$  and biexciton (XX) complexes. All the results described in the following section are obtained maximizing the carrier injection in the QD (i.e. the  $X^*$  emission).

### 3. Results and discussion

The energy level scheme characteristic of the QD is schematically displayed on figure 1 (a). This figure compiles a series of PL spectra obtained after HeNe excitation. At low powers the spectra is dominated by X recombination. The increase of excitation power leads to the consecutive predominance of  $X^*$ , XX, and finally, at the highest powers used, the atomic shell-like emission. The same lines can be identified when the QD PL is detected with the streak camera, as shown in figure 1(b), where the time-integrated PLs for increasing pump laser power are plotted. The X recombination appears at 776 nm (1.5977 eV) and does not shift significantly increasing power, nor do the rest of the excitonic transitions:  $X^*$  at 777.39 nm (1.5949 eV) and XX at 777.64 nm (1.5944 eV). Therefore we extract the binding energy of an extra electron to the exciton (2.86 meV) and the bi-exciton binding energy (3.36 meV).

Time-resolving the single QD PL is a remarkable challenge both in terms of detection sensibility and setup stability. Therefore it is necessary to work using the photon counting mode of the streak

camera. Figure 2(a) displays a streak camera image obtained after 15000 acquisitions of 222 ms for 105  $\mu\text{W}$  pump power. The same X, X\* and XX lines appear in the time-resolved spectrum, allowing us to extract the time evolution traces of each transition. These traces are summarized in figure 2(b) (X in red, X\* in blue) for different pump powers. Since the traces are rather noisy, in order to extract information about the recombination dynamics, it is necessary to smooth the curves, performing a 50 points adjacent averaging. Two characteristic times can be extracted from the smoothed time evolution traces: the time to reach the maximum emission intensity ( $t_{\text{max}}$ ) and the decay time ( $t_d$ ). The former is obtained directly from the curves, the later is found fitting the decaying part of the trace with a mono-exponential decay function. Such a qualitative analysis allows us to quickly compare the relaxation dynamics of X and X\* for different pump powers.

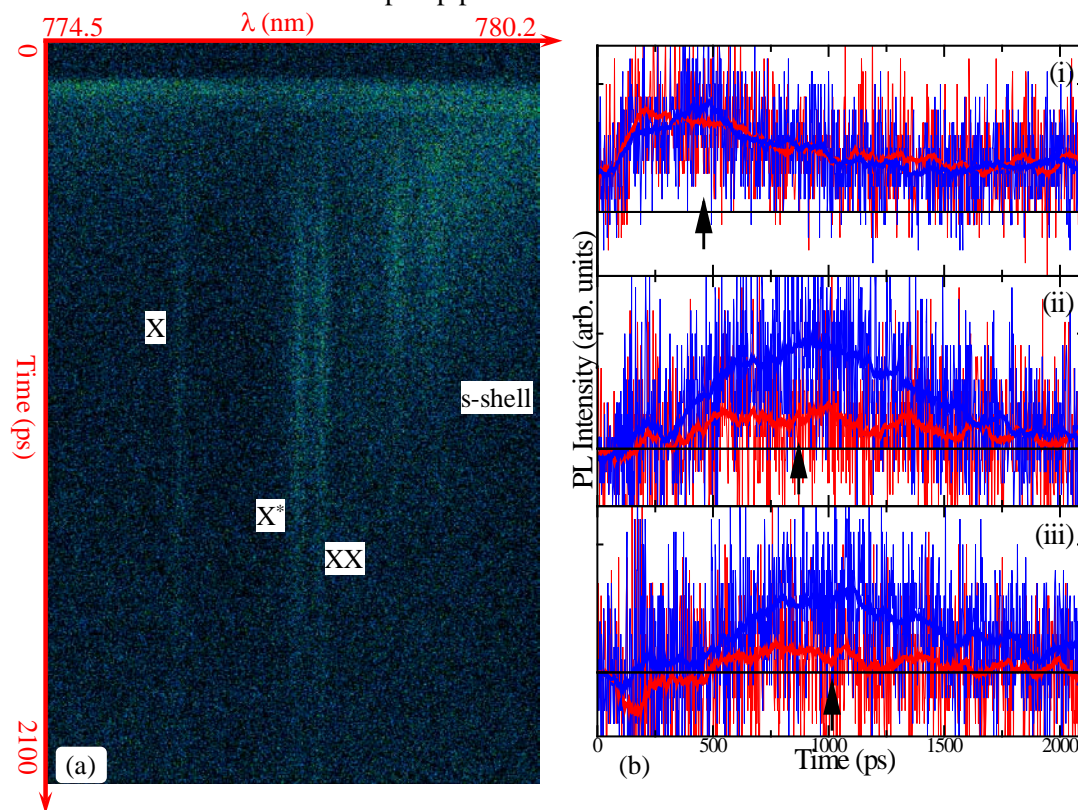


**Figure 2.-** (a) Streak camera image obtained after 15000 acquisitions of 222 ms for 105  $\mu\text{W}$  pump power. (b) Time evolution traces of X (in red) and X\* (in blue) recombination. Thin lines are the traces extracted directly from the streak camera images. Thick lines are the result of a 50 adjacent points averaging of the previous curves. The arrows in each graph indicate the position of the maximum emission intensity. The Ti:Al<sub>2</sub>O<sub>3</sub> pump powers used are (i) 32  $\mu\text{W}$ , (ii) 105  $\mu\text{W}$  and (iii) 200  $\mu\text{W}$ , respectively.

The first noticeable effect of the increase of pump power is revealed by  $t_{\text{max}}$ , which almost doubles rising the power by one order of magnitude (see the arrows in figure 2(b)). This is due to the fact that, at high powers, the dot is filled with carriers, so that recombination at early times occurs from the atomic-like shells and not from bound states. Only after the dot has emptied enough, reducing the carrier density and the screening, can electrons and holes start to interact and form bound states. At these intermediate times, there are still extra carriers in the dot and so the X\* and the XX lines become more intense. Once the X\* and XX emission channels are opened the dot is emptied rather quickly and there are not much carriers left to populate the X state. Hence the very small emission intensity at the X energy and the very long  $t_{\text{max}}$ .

The higher the pump power the larger the carrier density inside the dot and the longer it takes for the X complexes to reach their maximum emission intensity. This is corroborated by the streak camera image displayed in figure 2(a), since the maximum X\*/XX emission is reached only after the s-shell emission has almost finished.

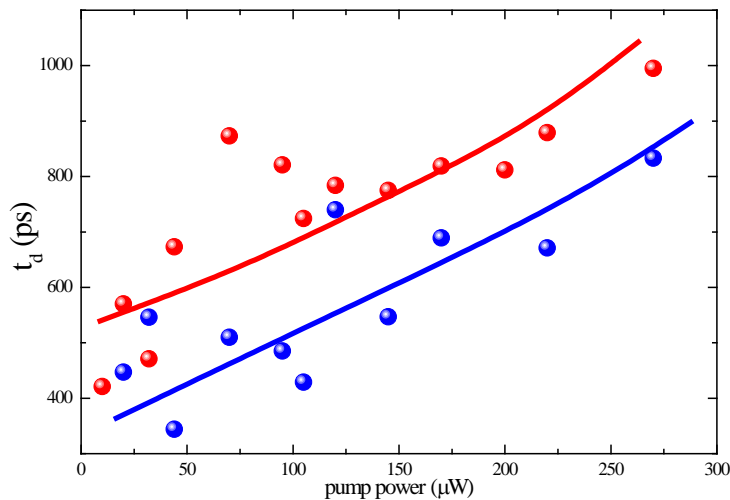


**Figure 3.-** PL decay time ( $t_d$ ), extracted from a fit with a mono-exponential decay, as a function of the Ti:Al<sub>2</sub>O<sub>3</sub> pump power for the X (in red) and the X\* (in blue) transition. The lines are guides to the eye.

The decay time, extracted from a mono-exponential decay function, shows a similar behavior, increasing with pump power. It almost doubles rising the pump power by one order of magnitude. Figure 3 summarizes the pump power dependence of  $t_d$  for both, X and X\* transitions. This retardation of the dynamics is due to the accumulation of carriers, which hinders the binding of electrons and holes and hence the formation and recombination of excitonic complexes.

These results show a remarkable difference when compared to the time-resolved results obtained with optical excitation above the barriers [3]. Even though the recombination sequence is maintained (first s-shell emission, then excitonic complexes), the decay time does not change significantly with excitation power. This difference is probably due to the fact that the recombination dynamics in the “above the barrier” case is governed by carrier diffusion and trapping. It is known that the diffusion of carriers is enhanced by the increase of pump power but the power dependence of carrier trapping processes is not so clear.

#### 4. Conclusions

We have time-resolved the PL emission of a single QD excited below the barriers, suppressing the influence of diffusion and trapping of carriers on the recombination dynamics. The large 3D confinement of our dots allows us to observe multi-excitonic complexes, such as the charged exciton (X\*) and the bi-exciton (XX), together with atomic-like shells (s, p and d). The increase of the carrier density confined inside the QD (increase of the pump power) is directly reflected by the PL spectrum and its dynamics: atomic-like shell emission at early times, then excitonic complexes (X\* and XX) and finally X. The presence of extra charges slows down the relaxation of X, X\* and XX since they can only become evident once the dot has emptied. This retardation is evidenced by both, the time of maximum emission intensity and the decay time.

#### Acknowledgements

This work was partially supported by the Spanish MEC (MAT2008-01555 and QOIT-CSD2006-00019) and the CAM (S2009/ESP-1503). MDM acknowledge financial support from the Ramon y Cajal programme.

#### References

- [1] Michler P, Kiraz A, Becher C, Schoenfeld W V, Petroff P M, Zhang L, Hu E and Imamoglu A 2000 *Science* **290** 2282  
Akopian N, Lindner N H, Poem E, Berltzky Y, Avron J and Gershoni D 2006 *Phys. Rev. Lett.* **96** 130501

- [2] Kong L M Cai J F, Wu Z Y, Gong Z, Niu Z C and Feng Z C 2006 *Thin Sol. Films* **498** 188  
Alder F, Geiger M, Bauknecht A, Scholz F, Schweizer H Pilkuhn M H, Ohnesorge B and Forchel A 1996 *J. Appl. Phys.* **80** 4019
- [3] Pietka B 2000 PhD Thesis *Excitonic Complexes in Natural Quantum Dots Formed in Type II GaAs/AlAs Structures* (Grenoble, France)